JGR Atmospheres

RESEARCH ARTICLE
10.1029/2024JD040869

Climate Impacts of the Millennium Eruption of Changbaishan Volcano

Y. Y. Yang[1,2,3], F. Shi[1], Z. F. Guo[1], W. Liu[4], H. H. Xue[4], Z. H. Zhuo[5], C. Q. Sun[1], C. Y. E[2], and Z. T. Guo[1,3]

[1]State Key Laboratory of Lithospheric and Environmental Coevolution, Institute of Geology and Geophysics, Chinese Academy of Sciences, Beijing, China, [2]Qinghai Province Key Laboratory of Physical Geography and Environmental Process, College of Geographical Science, Qinghai Normal University, Xining, China, [3]College of Earth and Planetary Sciences, University of Chinese Academy of Sciences, Beijing, China, [4]Georges Lemaître Centre for Earth and Climate Research, Earth and Life Institute, Université Catholique de Louvain, Louvain-la-Neuve, Belgium, [5]Department of Geosciences, University of Oslo, Oslo, Norway

Abstract The Millennium Eruption of Changbaishan Volcano is heralded as one of the largest explosive eruptions in the Late Holocene and produced huge quantities of tephra. The petrogeochemical method estimates that the Millennium Eruption emitted up to 45 Tg of sulfur into the atmosphere—more than in the Tambora eruption in 1815 CE, which caused "a year without a summer" across the Northern Hemisphere in 1816 CE. Despite such massive emissions, evidence for this eruption's climate impact in East Asia remains elusive. To explain this contradiction, this study used 67 high-resolution tree-ring-width records from the Northern Hemisphere spanning the past two millennia, complemented by volcanic sensitivity experiments conducted with the Community Earth System Model. Results reveal a prevailing decreasing/negative trend in the proxy records during the potential eruption period, with 945 CE marking the most notable negative anomaly, suggesting that the Millennium Eruption likely occurred in 945 CE rather than 946 CE. Sensitivity experiments, corroborated by proxy records, demonstrate that the Millennium Eruption induced substantial negative temperature anomalies at middle and high latitudes, alongside an increase in Meiyu-Baiu-Changma precipitation in the middle and lower reaches of the Yangtze River and southwestern Japan and a decrease in precipitation in India, northern China, and the South China Sea in the first post-eruption year. This study offers a novel perspective on the climate impact of the Millennium Eruption, reconciling previous discrepancies regarding its climate impact.

Plain Language Summary About a thousand years ago, the Changbaishan volcano erupted with incredible force, ranking as one of the largest historical eruptions in the past 2000 yrs. Despite its size, evidence for this eruption's climate impact in East Asia has remained elusive. We delved into this mystery by examining detailed high-resolution proxy records and performing climate model simulations. Our findings suggest that the climate effects of the eruption may have been unexpectedly strong, with the Millennium Eruption potentially occurring in 945 CE that is earlier than previously thought. The Millennium Eruption triggered notable cooling at middle and high latitudes, increased Meiyu-Baiu-Changma precipitation in the middle and lower reaches of the Yangtze River and southwestern Japan, and reduced precipitation in India, northern China, and the South China Sea. This research helps us understand how large volcanic eruptions can interact with other natural factors to influence our climate.

Key Points:

- Sulfur emissions of the Millennium Eruption estimated from a petrogeochemical method are inconsistent with the signal from ice-core samples
- A consistent negative response in the high-resolution paleoclimate records suggests a significant climate impact of the Millennium Eruption
- The eruption enhanced the Meiyu-Baiu-Changma precipitation while diminishing precipitation in India, northern China, and the South China Sea

Supporting Information:

Supporting Information may be found in the online version of this article.

Correspondence to:

F. Shi,
shifeng@mail.iggcas.ac.cn

Citation:

Yang, Y. Y., Shi, F., Guo, Z. F., Liu, W., Xue, H. H., Zhuo, Z. H., et al. (2024). Climate impacts of the Millennium Eruption of Changbaishan Volcano. *Journal of Geophysical Research: Atmospheres*, *129*, e2024JD040869. https://doi.org/10.1029/2024JD040869

Received 27 JAN 2024
Accepted 27 JUN 2024

Author Contributions:

Conceptualization: F. Shi, W. Liu
Data curation: Y. Y. Yang, W. Liu, H. H. Xue
Formal analysis: Y. Y. Yang
Methodology: Y. Y. Yang, F. Shi, W. Liu
Project administration: F. Shi, Z. T. Guo
Resources: F. Shi, Z. T. Guo
Supervision: F. Shi
Visualization: Y. Y. Yang
Writing – original draft: Y. Y. Yang
Writing – review & editing: Y. Y. Yang, F. Shi, Z. F. Guo, W. Liu, H. H. Xue, Z. H. Zhuo, C. Q. Sun, C. Y. E

1. Introduction

Volcanic eruption, an energy exchange process in the Earth's multi-layer system, is one of the most significant natural drivers of climate variability. It has a substantial impact on global climate change on interannual–interdecadal timescales by injecting materials such as sulfides, halides, and volcanic ash into the atmosphere (Blake, 2003; Robock, 2000).

The tectonic background of Cenozoic volcanism in China can be divided into the western Tethys tectonic domain associated with the India–Eurasia collision and the eastern Pacific deep subduction tectonic domain. As the main region of both the Pacific Rim volcanic belt and the distribution of Cenozoic volcanoes, the Eastern Volcanic Zone exhibits extensive lava coverage and possesses unique characteristics in its mantle source region (Chen et al., 2017; Liu et al., 1995). Located on the border between China and North Korea (41.98°N, 128.08°E),

Table 1
Compilation of Dating Results for the Millennium Eruption

Method	Material	Age	Reference
Ice-core chronologies	NEEM-2011-S1 ice core	940–942 CE	(Sun et al., 2014)
	GISP2 ice core	941–949 CE	
Accelerator mass spectrometry (AMS) ^{14}C dating	Carbonized logs	946–986 CE	(Jin et al., 2022)
	Larch tree log (*Larix*) with bark	943–949 CE	(Xu et al., 2013)
	Carbonized logs (*Larix*)	923–939 CE	(Yin et al., 2012)
	Charred trunks (*Larix and Juniperus sp.*)	945–960 CE 859–884 CE 935–963 CE	(Yatsuzuka et al., 2010)
^{14}C spike-matching method	Subfossil trunk (*mature Larix*) with bark	~946 CE	(Oppenheimer et al., 2017)
	Korean pine (*Pinus koraiensis*)	946–947 CE	(Hakozaki et al., 2018)

Changbaishan Volcano epitomizes Cenozoic intraplate volcanism in eastern China. It remains a site with potential for future eruption, as the hydrothermal activity and soil micro-seepage in the volcanic area are still vibrant (Liu et al., 2015; Wei et al., 2013; Zhang et al., 2018).

Geologic records reveal that Changbaishan volcanic activity initiated in the early Miocene, resulting in several significant eruptions, including the "Millennium Eruption" that occurred around 1000 CE (Liu et al., 2015; Sun et al., 2017; Wei et al., 2013; Yi et al., 2021; Zhang et al., 2018). This eruption ranks among the most intense eruptions of the Late Holocene and produced tephra that was widely distributed throughout Northeast Asia (Chen et al., 2016; Horn & Schmincke, 2000; McLean et al., 2016; Sun et al., 2014). It had an estimated VEI (Volcanic Explosivity Index) of 6–7 (Horn & Schmincke, 2000; Yang et al., 2021), comparable to the 1815 CE Tambora eruption known for triggering "the year without a summer" (53–58 Tg SO_2, VEI = 7) (Self et al., 2004). The far-reaching effects of such an eruption today could adversely affect atmosphere conditions, ecosystems, and human activities in East Asia; therefore, investigating the climate impact of the Millennium Eruption presents a crucial and relevant scientific endeavor.

Currently, there are two primary scientific controversies concerning the Millennium Eruption. The first pertains to its precise timing (Table 1). Despite the application of sophisticated dating methods such as electron probe single-shard analysis of volcanic glass, tephra layers in ice cores, and extensive radiocarbon dating of carbonized logs from ash deposits, an exact age for this eruption remains uncertain. Estimates vary widely, suggesting an eruption year between 943 and 948 CE, which presents a significant challenge for researchers attempting to understand the eruption's historical context and its impact on global climate. Recent work used the ^{14}C spike-matching method to date the Millennium Eruption to 946 CE based on the 775 CE ^{14}C spike events (Miyake et al., 2012; Oppenheimer et al., 2017). The subsequent study supported the results based on two Korean pine samples (Hakozaki et al., 2018). The ^{14}C peak event of 775 CE has been verified by numerous independent studies. However, the signal of the 775 CE peak does not occur simultaneously in the samples worldwide. For example, data from the Siberian and Altai records note a 775 CE peak but show a ^{14}C rise beginning 1 yr earlier, while New Zealand kauri data indicate a peak delayed by half a year (Park et al., 2017). This discrepancy suggests that even well-replicated composite-ring-width chronologies, precisely dated at an annual resolution, may sporadically deviate. Therefore, validation of these results is essential to correctly ascertain the eruptive year.

Historical documents are also employed to narrow down the dating of the Millennium Eruption, but these documents are not without their issues. They often contain exaggerated descriptions of natural phenomena and ambiguous references that may or may not pertain to volcanic eruptions. For example, the Koryŏsa (which describes the history of the Koryŏ dynasty) states, "That year the sky rumbled and cried out, there was an amnesty" in 946 CE (Hayakawa & Koyama, 1998), describing the sounds of volcanic eruptions. Similarly, the Nihon Kiryaku and Teishin Koki chronicles from Kyoto mention a "sound like thunder has resounded in the sky on February 7, 947 CE" (Hakozaki et al., 2018). These two documents have been proposed as potential indicators of the Millennium Eruption. However, the inconsistencies in the dates pose a challenge. Moreover, considering the frequent occurrence of volcanic disasters in Japan, the records available in Kyoto could not unequivocally be associated with the occurrence of the Millennium Eruption.

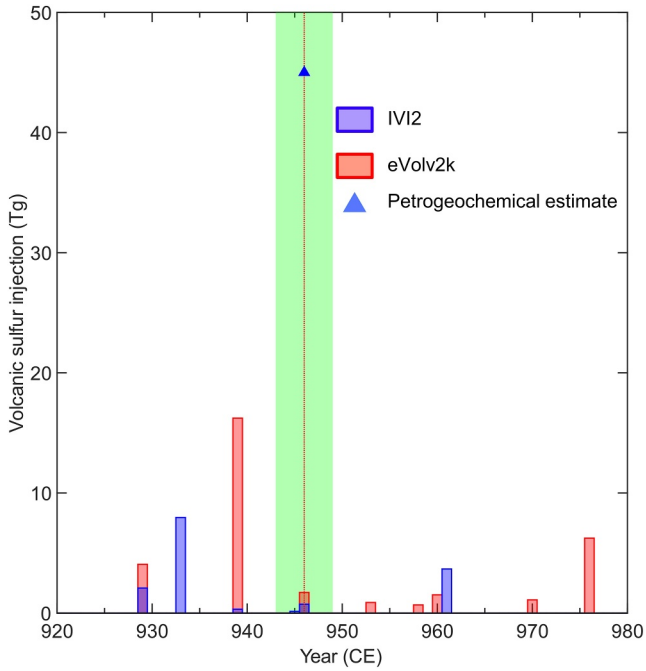

Figure 1. Comparison of volcanic sulfur emissions in 920–980 CE. The red histogram is the ice core–inferred volcanic stratospheric sulfur injection data (Toohey & Sigl, 2017), and the blue histogram indicates the sulfur aerosol-concentration reconstructions (Gao et al., 2008). The blue triangle represents the Millennium Eruption sulfur emissions, as estimated by the petrogeochemical method (Iacovino et al., 2016). The green shaded area denotes the potential eruption year of the Millennium Eruption, with the red dashed line corresponding to the year 946 CE.

The second point of contention is a stark contrast between the estimated sulfur emissions from the Millennium Eruption as deduced by the petrogeochemical methods and the sulfate fluxes recorded in ice cores. The petrogeochemical method (Iacovino et al., 2016) reveals that the Millennium Eruption emitted approximately 45 Tg of sulfur. As a significant silicic eruption, the eruption columns of the Millennium Eruption would have reached heights of ∼30–40 km, well above the tropopause at ∼12 km at this latitude (Costa et al., 2024), which indicates that there should be a substantial injection of stratospheric volcanic sulfur. However, the modest glacial sulfate signals recorded in reconstructed volcanic forcing IVI2 (Gao et al., 2008) and eVolv2k (Toohey & Sigl, 2017) (i.e., 0.74 Tg sulfur and 1.72 Tg sulfur) are much less significant than in the petrogeochemical data (Figure 1). To reconcile the contradictions mentioned above, this study examined high-resolution proxy records of the past 2000 yrs in the Northern Hemisphere and utilized the Community Earth System Model (CESM) to conduct volcanic sensitivity experiments.

2. Data and Methods

2.1. High-Resolution Proxy Data

The screening criteria of the proxy records (a) ensure accurate dating with an annual resolution; (b) encompass the period of 901–1000 CE; and (c) correlate instrumental temperature data (1901–2022 CE) with the nearest grid point that passes the significance test of $p < 0.05$. All records are normalized to a standard interval of [−1, 1]. The final dataset includes 67 tree-ring-width records, with a geographical spread across Asia, Canada, Europe, and the USA (Figure 2a). Moreover, the multi-proxy reconstructions involve the Yamalia region (Yamal Peninsula and Polar Urals) summer (June to July, JJ) temperature anomaly reconstructions (Briffa et al., 2013), and the reconstructed June-July-August (JJA) self-calibrating Palmer Drought Severity Index (Cook et al., 2015).

2.2. Sensitivity Experiment

Volcanic eruptions emit sulfide gases and aerosols, which are pivotal in instigating short-term climate variations due to their ability to modify solar radiation patterns. This, in turn, influences regional and global temperatures and alters atmospheric and hydrological dynamics (Pollack et al., 1976). A meticulous assessment of aerosol injections, defined by various sources, is essential not only for understanding historical volcanic climate effects but also for reconciling the discrepancies between sulfur emissions calculated by petrogeochemical evidence and sulfate aerosol fluxes recorded in ice cores.

The localized petrological evidence provides a more focused and direct approach for quantifying volcanic activity compared to distant ice-core records. Furthermore, the discrepancy between sulfur emissions estimated from petrogeochemical evidence and those from ice-core records is most pronounced and unusual in the case of the Changbaishan Millennium Eruption, particularly when compared with other eruptions, such as the 1257 CE Samalas eruption and 1783 CE Laki eruption. Therefore, we rescale the volcanic stratospheric injection based on some large and well-recognized volcanic events (i.e., 1257 CE (Vidal et al., 2016), 1783 CE (Thordarson & Self, 2003), and 1815 CE (Self et al., 2004)). Specifically, we compared volcanic stratospheric sulfur emissions recorded in ice cores (Gao et al., 2008) with those determined by petrogeochemical methods (Crisp & Spera, 1987; Devine et al., 1984; Fierstein & Nathenson, 1992). We then calculated the ratios (Table S2 in Supporting Information S1), which were 82% for Experiment 1, 38% for Experiment 2, and 99% for Experiment 3. Based on these ratios, we converted the potential stratospheric sulfur emissions from the Millennium Eruption. We also considered the possibility that some pre-eruption gases might have been released through passive degassing, which, due to their low energy, likely did not significantly influence the climate. Furthermore, considering that syn-eruptive sulfur-containing gases may not fully inject volatiles into the stratosphere (Horn &

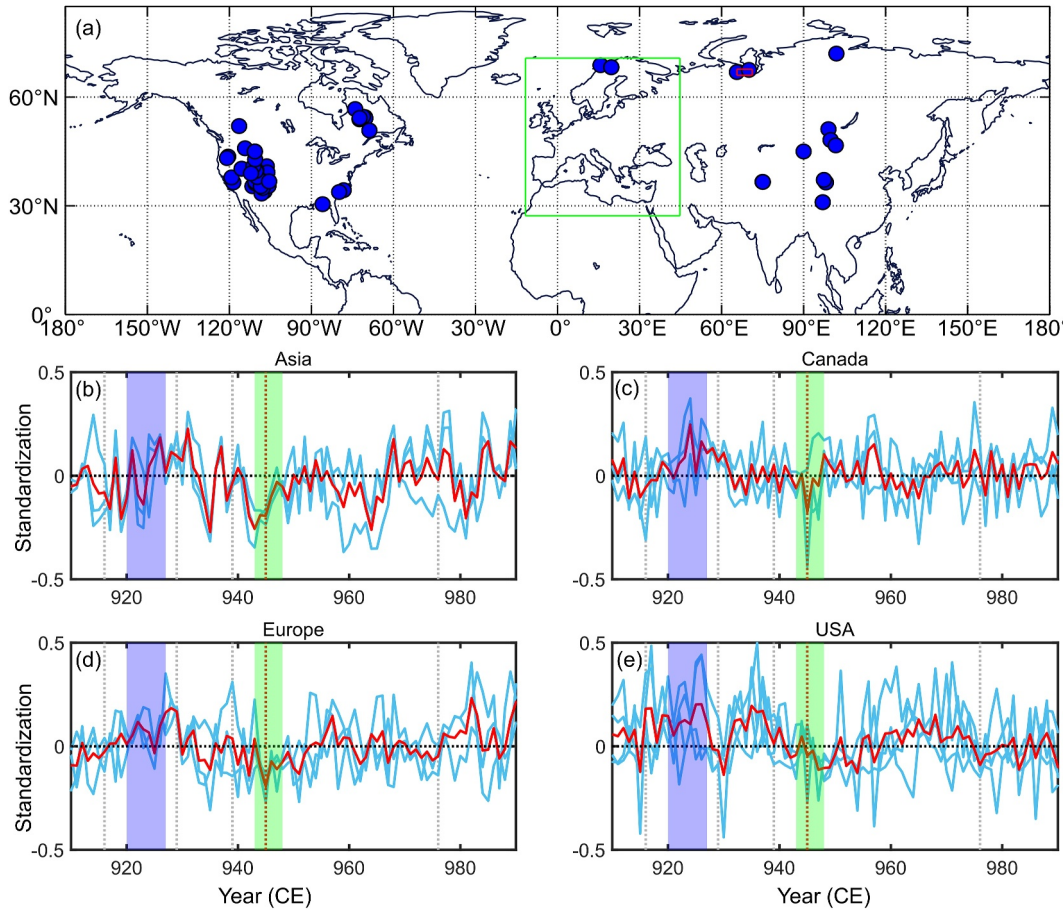

Figure 2. Spatial distribution of proxy records and their climate responses to the Millennium Eruption. (a) Geographical distribution of proxy records (b)–(e) Climate responses of the proxy records, with the blue dots indicating tree-ring-width records, the red box indicating the data coverage of the Yamalia region (Yamal Peninsula and Polar Urals) summer (June–July) temperature anomaly reconstructions (Briffa et al., 2013), and the green box indicating the data coverage of the reconstructed JJA self-calibrating Palmer Drought Severity Index (Cook et al., 2015). The blue lines are the standardized value of the proxy records, and the red lines are the averages of the standardized values. The red dashed lines correspond to the year 945 CE, while the gray dashed lines represent the volcanic eruption events during 910–990 CE. The green shades represent the potential eruption year, while purple shades denote the referenced climatological period without a volcanic eruption.

Schmincke, 2000; Iacovino et al., 2016; Lu et al., 1995), we focused our analysis on Experiment 1 and Experiment 2.

We refined our estimates for the eruption date and rescaled the stratospheric sulfur injection from 1.72 Tg to 36 Tg (Experiment 1) and 17 Tg (Experiment 2) based on the eVolv2k volcanic stratospheric sulfur injection database (Sigl et al., 2015, 2022; Toohey & Sigl, 2017). To generate the volcanic forcing, we utilized the Easy-Volcanic-Aerosol model (Toohey et al., 2016), as recommended by the Volcanic Forcings Model Intercomparison Project (VolMIP). Our simulations span a decade, from 945 to 954 CE; the horizontal resolution is 0.9° latitude and 1.25° longitude for the atmosphere component, and the grid of the ocean component is gx1v7 (CESM nominal 1° grid).

Moreover, we compared the volcanic sensitivity experiment with single volcanic forcing simulations (referred to as volcanic-only simulations) in the Community Earth System Model-Last Millennium Ensemble (CESM-LME) Project to evaluate the climate effects of the Millennium Eruption. This dataset, including five members, uses the original version of the IVI2 ice-core-derived volcanic sulfate mass-loading reconstruction (Gao et al., 2008). In the CESM-LME simulation, volcanic aerosols are modeled within the bottom three layers of the stratosphere and are designated as a uniform particle size distribution (Otto-Bliesner et al., 2016).

Table 2
Total Number of Proxy Records and the Proportion With a Negative Response During the Potential Volcanic Eruption Period

Region	Number of proxy records	Negative response ratio (%)
Asia	9	33
Canada	10	30
Europe	7	43
USA	41	10

3. Results

3.1. Variations of the Proxy Records

We performed a statistical analysis of the proxy records. Using IVI2 and eVolv2k as benchmarks, we defined 920–927 CE as a reference period without volcanic eruptions, and we defined the 943–948 CE period as including the Millennium Eruption's potential eruption year. Compared to the average values of the data from the reference period and the Millennium Eruption dating period, the results suggest a significant decline in tree-ring-width records only after the Millennium Eruption (Table 2). Regionally, Europe showed the greatest negative response, with 42% of the records showing reduced tree-ring widths, closely followed by Asia with 33% (Figure 2), which was statistically significant above the 90% confidence level according to a bootstrap test.

To determine whether fluctuations in these selected proxy records can be attributed to volcanic forcing, we evaluated the variables of these proxy records to the volcanic eruption during 1300–1900 CE, which exhibited distinct anomalies after the Millennium Eruption. Considering the potential uncertainty surrounding the chronology of paleovolcanic eruptions as well as the fact that one or more events might have an outsized leverage on the mean response value across epochs, we selected 21 volcanic eruption events with the volcanic stratospheric sulfur injection (VSSI) ranging from 3 Tg to 20 Tg based on the eVolv2k dataset (Figure S1 in Supporting Information S1, Table S3 in Supporting Information S1), and conducted a double-bootstrapped superposed epoch analysis to evaluate the impact of volcanic eruptions on post-volcanic proxy records in a probabilistic framework (Rao et al., 2019). This evaluation helped confirm the capability of these selected proxy records to accurately reflect signals of volcanic influence and the magnitude of declines during events with typical proven volcanic forcing. The results of the superposed epoch analysis show a negative trend in tree-ring-width records distributed in Asia, Canada, and Europe after the eruption (Figure 3). The distribution of proxy records in the USA differs slightly, which not only did the percentage of proxy records with negative anomalies for the Millennium Eruption appear to be minimal (10%, Table 2), but the negative response to the eruption occurred only in the year of the

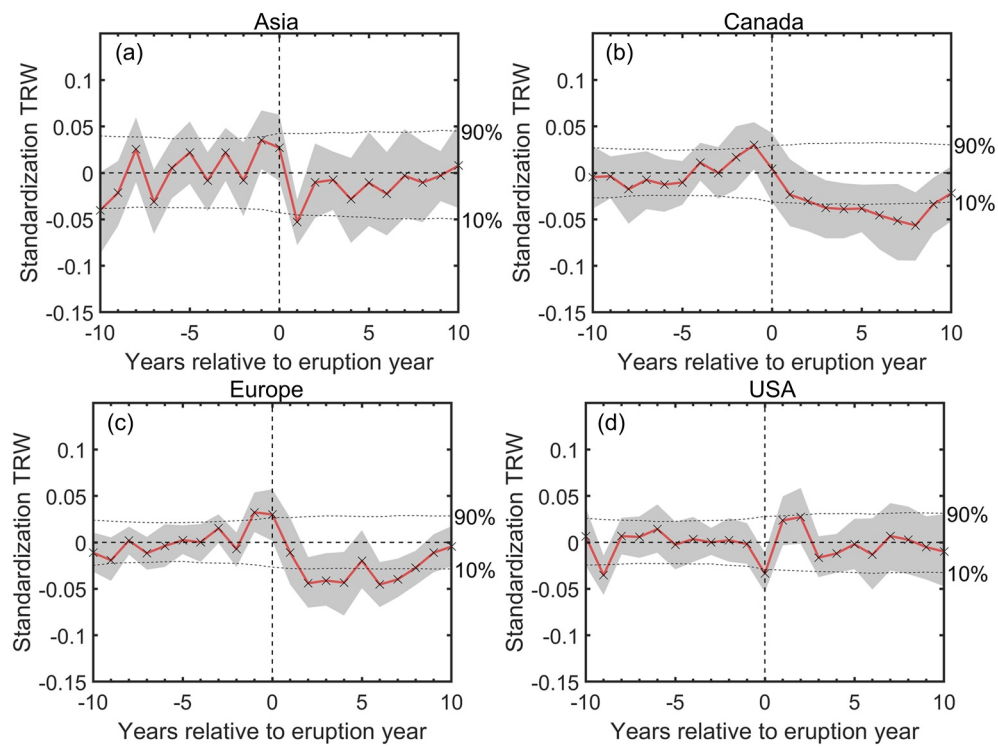

Figure 3. Climate response of proxy records to other volcanic eruptions (a–d) Tree-ring-width variations across Asia, Canada, Europe and the USA after the volcanic eruption.

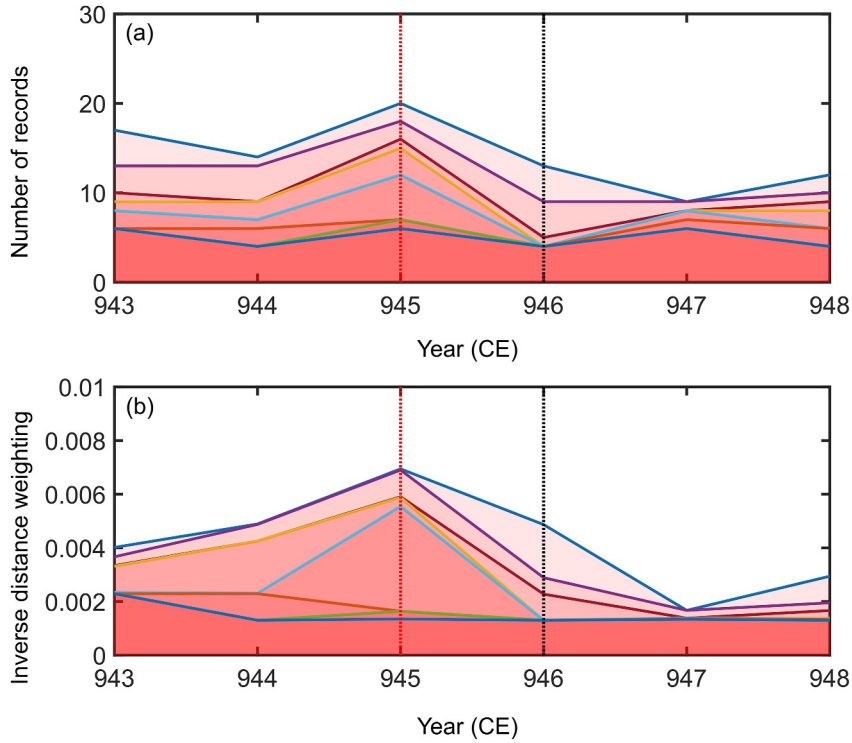

Figure 4. Year count analysis of tree-ring-width responses: (a) Number of records with a negative response during the potential eruption period. (b) Inverse Distance Weighting (IDW) calculation of records with negative responses. The number of records with negative responses, ranging from −0.1 to −0.24, is depicted by varying shading depths. Dashed red and black lines denote the years 945 CE and 946 CE, respectively.

eruption. Overall, the selected records exhibit significantly narrower rings in most regions after these eruptions. This supports the hypothesis that the negative anomalies in the tree-ring-width data are reflective of volcanic forcing.

To further quantitatively evaluate the response of proxy records to the Millennium Eruption, we examined the annual values of tree-ring widths during the volcanic eruption period in comparison to the reference climatological period without a volcanic eruption (Figure 4). The counts of significantly negative anomalies (anomaly ≤ −0.1 and passing a bootstrap test) in proxy records were 20 and 13 in 945 CE and 946 CE, respectively. To enhance the reliability of the results, we calculated the averaged Euclidean distances of the records from Changbaishan Volcano across four regions and weighted the previous results using the Inverse Distance Weighting (IDW) method. The results show that the peak negative response in the Northern Hemisphere tree-ring widths occurred in 945 CE. Notably, the quaternary chronology recognized the Millennium Eruption year in 946 CE with an IDW value of about 0.005, which is less than the IDW value of 0.007 in 945 CE (Figure 4b). Moreover, the integrated homogeneous grid data indicated a negative temperature anomaly trend in 945 CE (Figure S2 in Supporting Information S1) based on the tree-ring records (Briffa et al., 2013). The self-calibrating Palmer Drought Severity Index reconstructions derived from tree-ring records (Cook et al., 2015) pointed to noticeable drought conditions in 944–945 CE. Conversely, the data for 946 CE did not exhibit a substantial shift (Figure S3 in Supporting Information S1).

3.2. Annual Temperature and Precipitation Changes

To enhance the comprehension of climate responses to volcanic forcing and reconcile the paradox between petrogeochemical estimates and ice-core estimates of sulfur emissions, we conducted the CESM volcanic sensitivity experiment based on petrogeochemical method estimates to explore the temperature and precipitation variations. Figure 5 shows that, following the eruption, the temperatures in the middle- and high-latitude regions of Experiment 1 and Experiment 2 significantly dropped, with this effect lasting for around 3 yrs. In stark contrast,

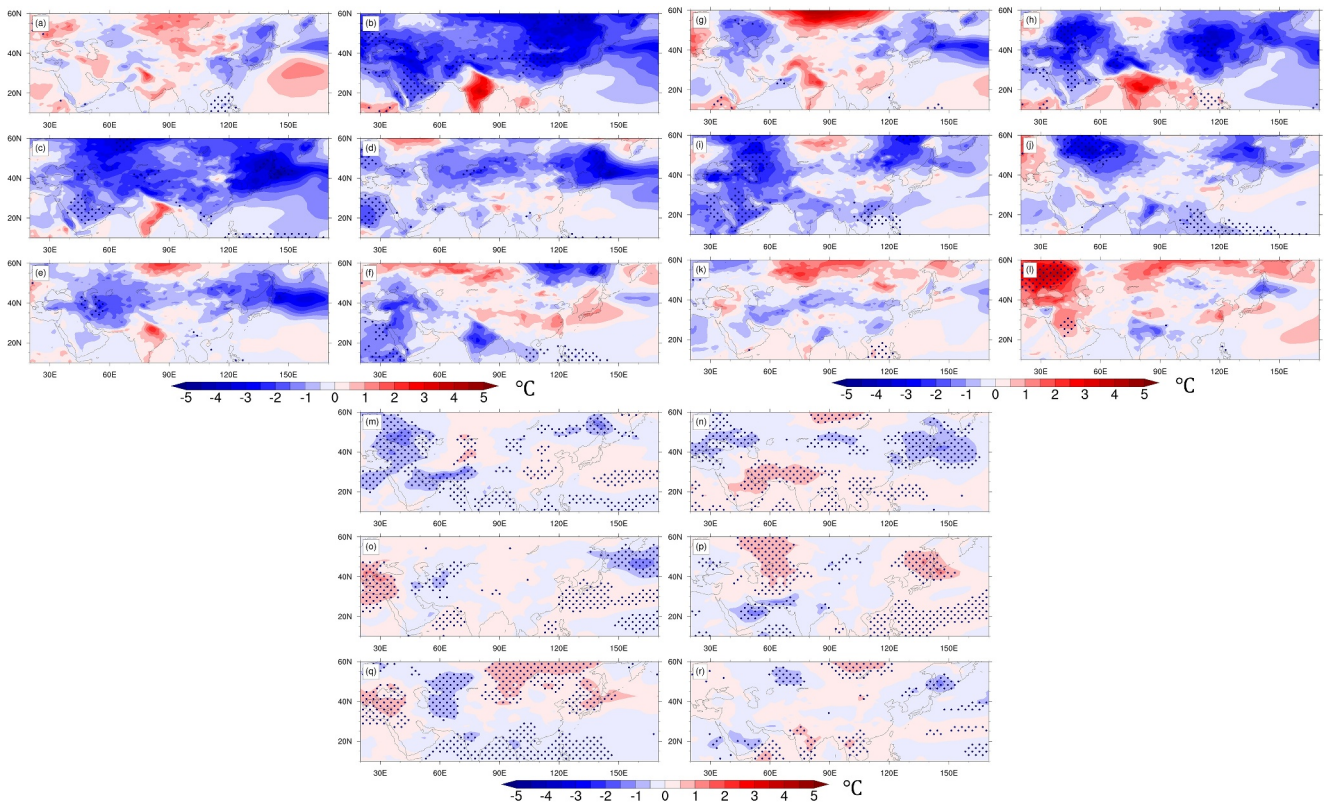

Figure 5. JJA temperature anomaly patterns during the volcanic period (a–f) Volcanic sensitivity Experiment 1 (g–l) Volcanic sensitivity Experiment 2 (m–r) CESM-LME volcanic single-forcing simulations. Stippling indicates temperature anomalies significant at the 90% confidence level.

the available CESM-LME volcanic eruption single-forcing simulations show no distinct anomalies following the eruption via ice core–based volcanic forcing findings.

The volcanic sensitivity simulations based on the petrogeochemical approach illustrated an initial increase in precipitation in the middle and lower reaches of the Yangtze River and southwestern Japan, accompanied by a decrease that was observed in India, northern China, and the South China Sea in the first post-eruption year. This pattern lasts for approximately 1–2 yrs following the eruption (Figure 6). Like the temperature results, the CESM-LME simulations show that the precipitation changes were likewise insignificant.

Overall, the volcanic sensitivity experiment reveals that the climate impact of the Millennium Eruption exhibits distinctive regional disparities. It is conceivable that cooling effects in middle and high latitudes may extend well beyond 2 to 3 yrs, while negative precipitation anomalies in the middle and low latitudes persist just 1 to 2 yrs. To elucidate the underlying mechanisms driving the spatial variability in the temperature and precipitation patterns, we analyzed the summer 850 hPa wind anomalies following the eruptions. The results suggest a weakening of the South Asian summer monsoon. The attenuation of the South Asian summer monsoon might be caused by the different response of the surface air temperatures over land and sea to the reduction of irradiation after volcanic eruptions, which leads to a reduced heating contrast between the ocean and land, thereby altering moisture transport and cloud formation processes (Chen et al., 2022; Gao & Gao, 2018; Liu, Xing, et al., 2022, Liu, Gao, et al., 2022; Peng et al., 2010; Sun et al., 2024; Zhuo et al., 2023).

4. Discussion

The enigma surrounding the Changbaishan Millennium Eruption consists of two main aspects: the difficulty in determining the eruption year and the associated mysterious climate impacts. In this study, proxy records and sensitivity experiments are used to provide a possible route to interpret these puzzles.

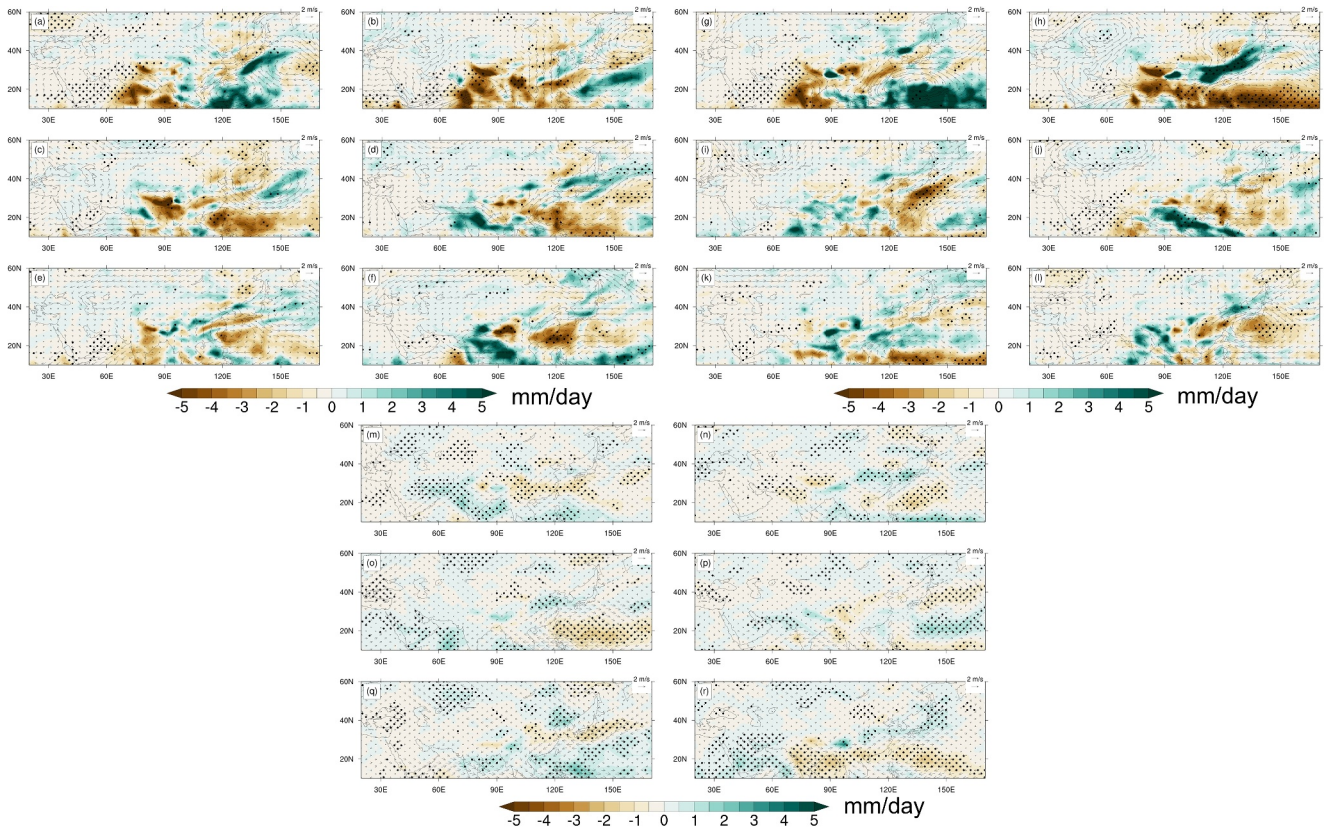

Figure 6. JJA precipitation anomaly patterns during the volcanic period (a–f) Volcanic sensitivity Experiment 1 (g–l) Volcanic sensitivity Experiment 2 (m–r) CESM-LME volcanic single-forcing simulations. Stippling indicates precipitation anomalies significant at the 90% confidence level.

Our analysis of high-resolution proxy records from the Northern Hemisphere indicates that the most pronounced narrowing of tree-ring widths occurred in 945 CE. Since tree-ring proxy records typically respond negatively to volcanic forcing, resulting in narrow tree-ring widths or absent rings (Anchukaitis et al., 2012; D'Arrigo et al., 2013; Gaoet al., 2023; Büntgen et al., 2022), and considering these proxies are influenced by both biological memory and growth strategies (i.e., the autocorrelated biological memory), the delay in tree radial growth is frequently detected following major volcanic eruptions, reflecting the climate and physiological conditions from the preceding year that affect subsequent tree-ring formation (Anchukaitis et al., 2012; Krakauer & Randerson, 2003). Consequently, the significant negative growth anomaly observed in 945 CE is likely a result of the extreme cold conditions experienced during the late growing season of the previous year. Thus, we postulate that the Millennium Eruption occurred between 944 and 945 CE.

Furthermore, there is a 1 yr discrepancy in the dating of the Millennium Eruption between historical documents from North Korea in 946 CE (Hayakawa & Koyama, 1998) and Japan in 947 CE (Hakozaki et al., 2018). These documents show a 1–2 yr gap when compared with the tree-ring data presented in Table 2. The extraordinary optic events in the atmosphere and stratospheric turbidity recorded could be indicative of a volcanic eruption (Guillet et al., 2023). Notably, atmospheric optical phenomena are generally more reliable indicators of volcanic eruptions than anomalous sound records. We found an item in the "The Second Annals of the Junior Emperor of Jin in the Old History of the Five Dynasties" that potentially signifies the occurrence of the Millennium Eruption. It is "日有黄白暈，二白虹夹日而行" which means "A yellowish-white halo appeared around the sun, two circumscribed halos alongside it" in February 944 CE (Zhang, 2004). This alignment with the tree-ring data (Table 2, Figure 3) corroborates our discussion on the chronology of the Millennial Eruption.

Both the proxy data and multi-proxy reconstructions reveal notable climatological anomalies in 944–945 CE that are particularly evident in Asia, Europe, and Canada. However, it is imperative to exercise caution in interpreting

this variability, as the anomalies observed in 945 CE may be confounded by internal variability within the climate system. In this regard, the SEA results provide valuable insights and suggest that the selected proxy records can reflect volcanic forcing. Given the variability in the records contained in the potential eruption period around 945 CE, we propose that the anomalies in the records indirectly correlate with the Millennium Eruption. It is noteworthy that the records exhibit myriad degrees of variability across different regions, indicating potential spatial heterogeneity in the volcanic climate effects.

Moreover, the volcanic climate impact is closely related to the injection and distribution of volcanic volatiles. The initial condition and climate state of the atmospheric circulation played an important role in the distribution of volcanic sulfate aerosols. For instance, the state of the polar vortex would affect the sulfate aerosols transport (Fuglestvedt et al., 2024). In addition, the Brewer-Dobson circulation (BDC) could have played a role in influencing the volcanic stratospheric sulfur transport and, thus, partially mitigated the climate effects. The BDC is a stratospheric equator-to-pole circulation that plays a crucial role in dispersing aerosols longitudinally and transporting them to higher latitudes (Brewer, 1949; Dobson & Massey, 1997; Roscoe, 2006). Since the latitude of Changbaishan Volcano is 42°N, it falls within the influence of shallow branches of the BDC characterized by downward directed streamlines, potentially impeding the dispersion of sulfate aerosols from the eruption (Tilmes et al., 2017). This disruption in dispersion may explain the contrast observed between the estimated sulfur emissions deduced by petrogeochemical methods and the sulfate fluxes recorded in ice cores. The localized effects of the BDC on aerosol transport and mixing near the Changbaishan volcano could result in deviations from expected atmospheric distribution patterns.

5. Conclusions

The Changbaishan volcano has garnered significant attention due to its distinct geological characteristics and its environmental and climate risks from potential future eruptions in East Asia. However, the indeterminate dating of the Millennium Eruption and its ambiguous climate response is still controversial. We sought to demystify the Millennium Eruption's climate response and refine its chronology through an integrated data-model comparison, utilizing Northern Hemisphere high-resolution proxy records, CESM volcanic sensitivity experiments, and CESM-LME simulations. Our major findings are summarized below.

1. The proxy records show a significant negative climate impact overall during the potential eruption dates, with the year 945 CE demonstrating the most pronounced negative response.
2. The sensitivity simulation based on petrogeochemical evidence indicates that the Millennium Eruption induced substantial negative temperature anomalies at middle and high latitudes, alongside increased Meiyu-Baiu-Changma precipitation in the middle and lower reaches of the Yangtze River and southwestern Japan, and decreased precipitation in India, northern China, and the South China Sea in the first post-eruption year.

Our volcanic sensitivity experiments are affected by several challenges with injection processes, sulfur-containing volatile gas transformations, and their stratosphere–troposphere transport. Future endeavors should employ the ASH Equilibrium Eulerian (ASHEE) model (Cerminara et al., 2016) and Whole Atmosphere Community Climate Model version six (Gettelman et al., 2019; Mills et al., 2016) for a refined numerical simulation of the Millennium Eruption's volcanic plumes and the transformation of stratospheric sulfate aerosols. We also emphasize the need for an enriched confluence of petrography, volcanic geochemistry, and climate model simulations to advance our understanding of volcanic climate effects and reveal the underlying mechanisms.

Conflict of Interest

The authors declare no conflicts of interest relevant to this study.

Data Availability Statement

The Community Earth System Model-Last Millennium Ensemble (CESM-LME) data are available at: https://www.earthsystemgrid.org/dataset/ucar.cgd.ccsm4.cesmLME.html. The ice core inferred volcanic stratospheric sulfur injection database (Toohey & Sigl, 2017) is available at: https://doi.org/10.1594/WDCC/eVolv2k_v2. The

ice-core-based volcanic atmospheric injection and loading dataset (Gao et al., 2008) can be obtained at: http://climate.envsci.rutgers.edu/IVI2. The Yamalia, northwest Siberia 1000 yr tree ring summer (June–July) temperature reconstruction (Briffa et al., 2013) is available at: https://www.ncei.noaa.gov/access/paleo-search/study/14468. The gridded (0.5 × 0.5°) reconstruction of droughts (Palmer Drought Severity Index, PDSI) for Europe and the Mediterranean region (Cook et al., 2015) is available at: https://www.ncei.noaa.gov/access/paleo-search/study/19419. The proxy-based records in this study can be freely accessed at the National Oceanic and Atmospheric Administration's (NOAA) National Centers for Environmental Information, and their download links are provided in Table S1 in Supporting Information S1.

Acknowledgments
We thank Professor Fei Xie for help with the discussion. This work was jointly funded by the Strategic Priority Research Program (Category B) of Chinese Academy of Sciences (Grant XDB0710000), National Natural Science Foundation of China (Grant 42077406), and the Key Research Program of the Institute of Geology and Geophysics, CAS (Grant IGGCAS-201905). Feng Shi is funded by the Youth Innovation Promotion Association CAS.

References

Anchukaitis, K. J., Breitenmoser, P., Briffa, K. R., Buchwal, A., Büntgen, U., Cook, E. R., et al. (2012). Tree rings and volcanic cooling. *Nature Geoscience*, *5*(12), 836–837. https://doi.org/10.1038/ngeo1645

Blake, S. (2003). Correlations between eruption magnitude, SO_2 yield, and surface cooling. *Geological Society*, *213*(1), 371–380. London, Special Publications. https://doi.org/10.1144/GSL.SP.2003.213.01.22

Brewer, A. W. (1949). Evidence for a world circulation provided by the measurements of helium and water vapour distribution in the stratosphere. *Quarterly Journal of the Royal Meteorological Society*, *75*(326), 351–363. https://doi.org/10.1002/qj.49707532603

Briffa, K. R., Melvin, T. M., Osborn, T. J., Hantemirov, R. M., Kirdyanov, A. V., Mazepa, V. S., et al. (2013). Reassessing the evidence for tree-growth and inferred temperature change during the Common Era in Yamalia, northwest Siberia (Vol. *72*, pp. 83–107). [Dataset]. https://doi.org/10.1016/j.quascirev.2013.04.008. *Quaternary Science Reviews*.

Büntgen, U., Smith, S. H., Wagner, S., Krusic, P., Esper, J., Piermattei, A., et al. (2022). Global tree-ring response and inferred climate variation following the mid-thirteenth century Samalas eruption. *Climate Dynamics*, *59*(1), 531–546. https://doi.org/10.1007/s00382-022-06141-3

Cerminara, M., Esposti Ongaro, T., & Berselli, L. C. (2016). ASHEE-1.0: A compressible, equilibrium–eulerian model for volcanic ash plumes. *Geoscientific Model Development*, *9*(2), 697–730. https://doi.org/10.5194/gmd-9-697-2016

Chen, H., Xia, Q. K., Ingrin, J., Deloule, E., & Bi, Y. (2017). Heterogeneous source components of intraplate basalts from NE China induced by the ongoing Pacific slab subduction. *Earth and Planetary Science Letters*, *459*, 208–220. https://doi.org/10.1016/j.epsl.2016.11.030

Chen, K., Ning, L., Liu, Z., Liu, J., Yan, M., Sun, W., et al. (2022). Nonlinear responses of droughts over China to volcanic eruptions at different drought phases. *Geophysical Research Letters*, *49*(4), e2021GL096454. https://doi.org/10.1029/2021GL096454

Chen, X. Y., Blockley, S. P. E., Tarasov, P. E., Xu, Y. G., McLean, D., Tomlinson, E. L., et al. (2016). Clarifying the distal to proximal tephrochronology of the millennium (B–Tm) eruption, Changbaishan Volcano, northeast China. *Quaternary Geochronology*, *33*, 61–75. https://doi.org/10.1016/j.quageo.2016.02.003

Cook, E. R., Seager, R., Kushnir, Y., Briffa, K. R., Büntgen, U., Frank, D., et al. (2015). Old world megadroughts and pluvials during the common era (Vol. *1*). [Dataset]. https://doi.org/10.1126/sciadv.1500561. *Science Advances* (10) e1500561.

Costa, A., Mingari, L., Smith, V. C., Macedonio, G., McLean, D., Folch, A., et al. (2024). Eruption plumes extended more than 30 km in altitude in both phases of the Millennium Eruption of Paektu (Changbaishan) volcano. *Communications Earth & Environment*, *5*(1), 1–13. https://doi.org/10.1038/s43247-023-01162-0

Crisp, J. A., & Spera, F. J. (1987). Pyroclastic flows and lavas of the mogan and fataga formations, tejeda volcano, gran canaria, canary islands: Mineral chemistry, intensive parameters, and magma chamber evolution. *Contributions to Mineralogy and Petrology*, *96*(4), 503–518. https://doi.org/10.1007/BF01166695

D'Arrigo, R., Wilson, R., & Anchukaitis, K. J. (2013). Volcanic cooling signal in tree ring temperature records for the past millennium. *Journal of Geophysical Research: Atmospheres*, *118*(16), 9000–9010. https://doi.org/10.1002/jgrd.50692

Devine, J. D., Sigurdsson, H., Davis, A. N., & Self, S. (1984). Estimates of sulfur and chlorine yield to the atmosphere from volcanic eruptions and potential climatic effects. *Journal of Geophysical Research*, *89*(B7), 6309–6325. https://doi.org/10.1029/JB089iB07p06309

Dobson, G. M. B., & Massey, H. S. W. (1997). Origin and distribution of the polyatomic molecules in the atmosphere. *Proceedings of the Royal Society of London - Series A: Mathematical and Physical Sciences*, *236*(1205), 187–193. https://doi.org/10.1098/rspa.1956.0127

Fierstein, J., & Nathenson, M. (1992). Another look at the calculation of fallout tephra volumes. *Bulletin of Volcanology*, *54*(2), 156–167. https://doi.org/10.1007/BF00278005

Fuglestvedt, H. F., Zhuo, Z., Toohey, M., & Krüger, K. (2024). Volcanic forcing of high-latitude Northern Hemisphere eruptions. *NPJ Climate and Atmospheric Science*, *7*(1), 1–12. https://doi.org/10.1038/s41612-023-00539-4

Gao, C., Robock, A., & Ammann, C. (2008). Volcanic forcing of climate over the past 1500 years: An improved ice core-based index for climate models (Vol. *113*). [Dataset]. https://doi.org/10.1029/2008JD010239. *Journal of Geophysical Research* (D23).

Gao, C. C., & Gao, Y. J. (2018). Revisited asian monsoon hydroclimate response to volcanic eruptions. *Journal of Geophysical Research: Atmospheres*, *123*(15), 7883–7896. https://doi.org/10.1029/2017JD027907

Gao, S., Camarero, J. J., Babst, F., & Liang, E. (2023). Global tree growth resilience to cold extremes following the Tambora volcanic eruption. *Nature Communications*, *14*(1), 6616. https://doi.org/10.1038/s41467-023-42409-w

Gettelman, A., Mills, M. J., Kinnison, D. E., Garcia, R. R., Smith, A. K., Marsh, D. R., et al. (2019). The Whole atmosphere community climate model version 6 (WACCM6). *Journal of Geophysical Research: Atmospheres*, *124*(23), 12380–12403. https://doi.org/10.1029/2019JD030943

Guillet, S., Corona, C., Oppenheimer, C., Lavigne, F., Khodri, M., Ludlow, F., et al. (2023). Lunar eclipses illuminate timing and climate impact of medieval volcanism. *Nature*, *616*(7955), 90–95. https://doi.org/10.1038/s41586-023-05751-z

Hakozaki, M., Miyake, F., Nakamura, T., Kimura, K., Masuda, K., & Okuno, M. (2018). Verification of the annual dating of the 10th century Baitoushan volcano eruption based on an AD 774–775 radiocarbon spike. *Radiocarbon*, *60*(1), 261–268. https://doi.org/10.1017/RDC.2017.75

Hayakawa, Y., & Koyama, M. (1998). Dates of two major eruptions from Towada and Baitoushan in the 10th century. *Bulletin of the Volcanological Society of Japan*, *43*(5), 403–407. https://doi.org/10.18940/kazan.43.5_403

Horn, S., & Schmincke, H. U. (2000). Volatile emission during the eruption of Baitoushan Volcano (China/North Korea) ca. 969 AD. *Bulletin of Volcanology*, *61*(8), 537–555. https://doi.org/10.1007/s004450050004

Iacovino, K., Ju-Song, K., Sisson, T., Lowenstern, J., Kuk-Hun, R., Jong-Nam, J., et al. (2016). Quantifying gas emissions from the "millennium eruption" of paektu volcano, democratic people's Republic of Korea/China. *Science Advances*, *2*(11), e1600913. https://doi.org/10.1126/sciadv.1600913

Jin, Y., Li, J., Zhao, Y., Xu, C., Chen, Z., Li, F., et al. (2022). Cambial evidence of the "Millennium Eruption" of Changbaishan volcano (c. 946 CE) and century-scale climatic change in the Middle Ages. *Palaeogeography, Palaeoclimatology, Palaeoecology*, *595*, 110971. https://doi.org/10.1016/j.palaeo.2022.110971

Krakauer, N. Y., & Randerson, J. T. (2003). Do volcanic eruptions enhance or diminish net primary production? Evidence from tree rings. *Global Biogeochemical Cycles*, *17*(4). https://doi.org/10.1029/2003GB002076

Liu, F., Gao, C., Chai, J., Robock, A., Wang, B., Li, J., et al. (2022). Tropical volcanism enhanced the East Asian summer monsoon during the last millennium. *Nature Communications*, *13*(1), 3429. https://doi.org/10.1038/s41467-022-31108-7

Liu, F., Xing, C., Chen, L., Gao, C., Lian, T., Zhou, S., et al. (2022). Relative roles of land and ocean cooling in triggering an El niño following tropical volcanic eruptions. *Geophysical Research Letters*, *49*(23), e2022GL100609. https://doi.org/10.1029/2022GL100609

Liu, J., Chen, S., Guo, Z., Guo, W., He, H., You, H., et al. (2015). Geological background and geodynamic mechanism of Mt. Changbai volcanoes on the China–Korea border. *Lithos*, *236–237*, 46–73. https://doi.org/10.1016/j.lithos.2015.08.011

Liu, R., Xie, G., Zhou, X., Chen, W., & Fan, Q. (1995). Tectonic environments of Cenozoic volcanic rocks in China and characteristics of the source regions in the mantle. *Chinese Journal of Geochemistry*, *14*(4), 289–302. https://doi.org/10.1007/BF02872628

Lu, F., Anderson, A. T., & Davis, A. M. (1995). Diffusional gradients at the crystal/melt interface and their effect on the compositions of melt inclusions. *The Journal of Geology*, *103*(5), 591–597. https://doi.org/10.1086/629778

McLean, D., Albert, P. G., Nakagawa, T., Staff, R. A., Suzuki, T., & Smith, V. C. (2016). Identification of the Changbaishan 'Millennium' (B-Tm) eruption deposit in the Lake Suigetsu (SG06) sedimentary archive, Japan: Synchronisation of hemispheric-wide palaeoclimate archives. *Quaternary Science Reviews*, *150*, 301–307. https://doi.org/10.1016/j.quascirev.2016.08.022

Mills, M. J., Schmidt, A., Easter, R., Solomon, S., Kinnison, D. E., Ghan, S. J., et al. (2016). Global volcanic aerosol properties derived from emissions, 1990–2014, using CESM1(WACCM). *Journal of Geophysical Research: Atmospheres*, *121*(5), 2332–2348. https://doi.org/10.1002/2015JD024290

Miyake, F., Nagaya, K., Masuda, K., & Nakamura, T. (2012). A signature of cosmic-ray increase in AD 774–775 from tree rings in Japan. *Nature*, *486*(7402), 240–242. https://doi.org/10.1038/nature11123

Oppenheimer, C., Wacker, L., Xu, J., Galván, J. D., Stoffel, M., Guillet, S., et al. (2017). Multi-proxy dating the 'millennium eruption' of changbaishan to late 946 CE. *Quaternary Science Reviews*, *158*, 164–171. https://doi.org/10.1016/j.quascirev.2016.12.024

Otto-Bliesner, B. L., Brady, E. C., Fasullo, J., Jahn, A., Landrum, L., Stevenson, S., et al. (2016). Climate variability and change since 850 CE: An ensemble approach with the community Earth system model. *Bulletin of the American Meteorological Society*, *97*(5), 735–754. https://doi.org/10.1175/BAMS-D-14-00233.1

Park, J., Southon, J., Fahrni, S., Creasman, P. P., & Mewaldt, R. (2017). Relationship between solar activity and Δ14C peaks in AD 775, AD 994, and 660 BC. *Radiocarbon*, *59*(4), 1147–1156. https://doi.org/10.1017/RDC.2017.59

Peng, Y., Shen, C., Wang, W. C., & Xu, Y. (2010). Response of summer precipitation over Eastern China to large volcanic eruptions. *Journal of Climate*, *23*(3), 818–824. https://doi.org/10.1175/2009JCLI2950.1

Pollack, J. B., Toon, O. B., Sagan, C., Summers, A., Baldwin, B., & Van Camp, W. (1976). Volcanic explosions and climatic change: A theoretical assessment. *Journal of Geophysical Research*, *81*(6), 1071–1083. https://doi.org/10.1029/JC081i006p01071

Rao, M. P., Cook, E. R., Cook, B. I., Anchukaitis, K. J., D'Arrigo, R. D., Krusic, P. J., & LeGrande, A. N. (2019). A double bootstrap approach to Superposed Epoch Analysis to evaluate response uncertainty [Software]. *Dendrochronologia*, *55*, 119–124. https://doi.org/10.1016/j.dendro.2019.05.001

Robock, A. (2000). Volcanic eruptions and climate. *Reviews of Geophysics*, *38*(2), 191–219. https://doi.org/10.1029/1998RG000054

Roscoe, H. K. (2006). The Brewer–Dobson circulation in the stratosphere and mesosphere – Is there a trend? *Advances in Space Research*, *38*(11), 2446–2451. https://doi.org/10.1016/j.asr.2006.02.078

Self, S., Gertisser, R., Thordarson, T., Rampino, M. R., & Wolff, J. A. (2004). Magma volume, volatile emissions, and stratospheric aerosols from the 1815 eruption of Tambora. *Geophysical Research Letters*, *31*(20). https://doi.org/10.1029/2004GL020925

Sigl, M., Toohey, M., McConnell, J. R., Cole-Dai, J., & Severi, M. (2022). Volcanic stratospheric sulfur injections and aerosol optical depth during the Holocene (past 11500 years) from a bipolar ice-core array. *Earth System Science Data*, *14*(7), 3167–3196. https://doi.org/10.5194/essd-14-3167-2022

Sigl, M., Winstrup, M., McConnell, J. R., Welten, K. C., Plunkett, G., Ludlow, F., et al. (2015). Timing and climate forcing of volcanic eruptions for the past 2,500 years. *Nature*, *523*(7562), 543–549. https://doi.org/10.1038/nature14565

Sun, C., Liu, J., You, H., & Nemeth, K. (2017). Tephrostratigraphy of Changbaishan volcano, northeast China, since the mid-Holocene. *Quaternary Science Reviews*, *177*, 104–119. https://doi.org/10.1016/j.quascirev.2017.10.021

Sun, C., Plunkett, G., Liu, J., Zhao, H., Sigl, M., McConnell, J. R., et al. (2014). Ash from Changbaishan Millennium Eruption recorded in Greenland ice: Implications for determining the eruption's timing and impact. *Geophysical Research Letters*, *41*(2), 694–701. https://doi.org/10.1002/2013GL058642

Sun, W., Chen, D., Lü, G., Ning, L., Gao, C., Zhang, R., et al. (2024). Impacts of major volcanic eruptions over the past two millennia on both global and Chinese climates: A review. *Science China Earth Sciences*, *67*(1), 61–78. https://doi.org/10.1007/s11430-022-1218-0

Thordarson, T., & Self, S. (2003). Atmospheric and environmental effects of the 1783–1784 Laki eruption: A review and reassessment. *Journal of Geophysical Research*, *108*(D1), AAC 7-1–AAC 7-29. https://doi.org/10.1029/2001JD002042

Tilmes, S., Richter, J. H., Mills, M. J., Kravitz, B., MacMartin, D. G., Vitt, F., et al. (2017). Sensitivity of aerosol distribution and climate response to stratospheric SO_2 injection locations. *Journal of Geophysical Research: Atmospheres*, *122*(23), 12591–12615. https://doi.org/10.1002/2017JD026888

Toohey, M., & Sigl, M. (2017). Reconstructed volcanic stratospheric sulfur injections and aerosol optical depth, 500 BCE to 1900 CE, version 2. [Dataset]. https://doi.org/10.1594/WDCC/eVolv2k_v2. *World Data Center for Climate (WDCC) at DKRZ.*

Toohey, M., Stevens, B., Schmidt, H., & Timmreck, C. (2016). Easy Volcanic Aerosol (EVA v1.0): An idealized forcing generator for climate simulations. *Geoscientific Model Development*, *9*(11), 4049–4070. https://doi.org/10.5194/gmd-9-4049-2016

Vidal, C. M., Métrich, N., Komorowski, J.-C., Pratomo, I., Michel, A., Kartadinata, N., et al. (2016). The 1257 Samalas eruption (lombok, Indonesia): The single greatest stratospheric gas release of the common era. *Scientific Reports*, *6*(1), 34868. https://doi.org/10.1038/srep34868

Wei, H., Liu, G., & Gill, J. (2013). Review of eruptive activity at tianchi volcano, changbaishan, northeast China: Implications for possible future eruptions. *Bulletin of Volcanology*, *75*(4), 706. https://doi.org/10.1007/s00445-013-0706-5

Xu, J., Pan, B., Liu, T., Hajdas, I., Zhao, B., Yu, H., et al. (2013). Climatic impact of the Millennium Eruption of Changbaishan volcano in China: New insights from high-precision radiocarbon wiggle-match dating. *Geophysical Research Letters*, *40*(1), 54–59. https://doi.org/10.1029/2012GL054246

Yang, Q., Jenkins, S. F., Lerner, G. A., Li, W., Suzuki, T., McLean, D., et al. (2021). The millennium eruption of changbaishan tianchi Volcano is VEI 6, not 7. *Bulletin of Volcanology*, *83*(11), 74. https://doi.org/10.1007/s00445-021-01487-8

Yatsuzuka, S., Okuno, M., Nakamura, T., Kimura, K., Setoma, Y., Miyamoto, T., et al. (2010). 14C wiggle-matching of the B-Tm tephra, baitoushan volcano, China/North Korea. *Radiocarbon*, *52*(3), 933–940. https://doi.org/10.1017/S0033822200046038

Yi, J., Wang, P., Shan, X., Ventura, G., Wu, C., Guo, J., et al. (2021). Modeling the multi-level plumbing system of the Changbaishan caldera from geochemical, mineralogical, Sr-Nd isotopic and integrated geophysical data. *Geoscience Frontiers*, *12*(5), 101171. https://doi.org/10.1016/j.gsf.2021.101171

Yin, J., Jull, A. J. T., Burr, G. S., & Zheng, Y. (2012). A wiggle-match age for the millennium eruption of tianchi volcano at changbaishan, northeastern China. *Quaternary Science Reviews*, *47*, 150–159. https://doi.org/10.1016/j.quascirev.2012.05.015

Zhang, D. E. (2004). *A compendium of Chinese meteorological records of the last 3,000 Years (in Chinese)* (pp. 2434–2454). Jiangsu Education Press.

Zhang, M., Guo, Z., Liu, J., Liu, G., Zhang, L., Lei, M., et al. (2018). The intraplate changbaishan volcanic field (China/North Korea): A review on eruptive history, magma genesis, geodynamic significance, recent dynamics and potential hazards. *Earth-Science Reviews*, *187*, 19–52. https://doi.org/10.1016/j.earscirev.2018.07.011

Zhuo, Z. H., Kirchner, I., & Cubasch, U. (2023). Mechanisms of hydrological responses to volcanic eruptions in the Asian monsoon and westerlies-dominated subregions. *Climate of the Past*, *19*(4), 835–849. https://doi.org/10.5194/cp-19-835-2023